Orbital: The Electronic Journal of Chemistry
journal homepage: www.orbital.ufms.br
e-ISSN 1984-6428

| Vol 11 | | No. 2 | | Special Issue April 2019 |

TECHNICAL NOTE

A Simple and Complete Supercapacitor Characterization System Using a Programmable Sourcemeter

José Henrique Alano[a], Lucas da Silva Rodrigues[a], Guilherme Kurz Maron[a], Bruno da Silveira Noremberg[a], Amanda Dantas de Oliveira[a], Oscar Paniz[a], Rubens Maribondo Do Nascimento[b], Neftalí Lenin Villarreal Carreño*[a]

[a]Graduate Program in Materials Science and Engineering, Technology Development Center, Federal University of Pelotas, Gomes Carneiro 1, Pelotas, RS, 96010-000, Brazil.
[b]Department of Materials Engineering, Technology Center, Federal University of Rio Grande do Norte, 1534, Natal, RN, 59078-970, Brazil.

Article history: Received: 19 December 2019; revised: 12 March 2019; accepted: 12 March 2019. Available online: 22 April 2019. DOI: http://dx.doi.org/10.17807/orbital.v11i2.1374

Abstract:

The development of new materials and systems capable of storing energy efficiently with a fast power delivering has been the subject of several studies. Many techniques and instruments are used for the characterization of these systems. Some involve the use of electrochemical techniques, such as cyclic voltammetry and electrochemical impedance spectroscopy, while others use instruments specially developed for this purpose. In this study, we provide a simple and functional supercapacitor characterization system using a programmable sourcemeter with an embedded scripting language. For the validation of the system, commercial capacitors and supercapacitors devices based on activated carbon and manganese dioxide were used. In a few steps, the system is capable of efficiently determine the main parameters used in the characterization of supercapacitors, for instance, specific capacitance, specific energy density, specific power density and equivalent series resistance. From the data collected, the system can also determine the stability and performance of supercapacitors, which are fundamental parameters used in the development of new electrodes for energy storage devices.

Keywords: electrochemical characterization; energy storage devices; programmable sourcemeter; supercapacitors

1. Introduction

Supercapacitors are energy storage devices (ESDs) that has been a matter of recurrent interest. Unlike batteries, which store energy through slow bulk redox reactions, supercapacitors store energy by ion adsorption or fast surface redox reactions [1, 2]. These storage mechanisms allows the use of these ESDs in applications that require high power delivery, such as in hybrid electric vehicles and portable electronics. As limitation, supercapacitors presents lower energy storage capacity than batteries [2, 3]. To outstanding this limitation, much effort has been made to overcome the levels of power, energy and stability of electrode materials currently used in supercapacitors.

Many methods have been used for the characterization of supercapacitors, the majority using testing instruments that run the manufacturer's system [4–6]. Depending on the brand and model of the equipment, the system does not allow existing routines to be modified or elaborated. On the other hand, there is an increasing trend in the use of testing instruments that have embedded processors and flexible programmability. These features allow the user to create their own routines or perform on-board tasks on the instrument. A full-featured embeddable scripting language, such as Lua, has been widely used in these types of instruments due to its portability and ease of integration with other programming languages [7, 8]. The use of scripting programs facilitates the experimental

*Corresponding author. E-mail: neftali@ufpel.edu.br

routine, since it allows the accomplishment of all the procedure in a batch, streamlining the process, minimizing arbitrary errors of data treatments and making all experiments standardized. In addition to these features, the system is an open source and can be modified and adapted to the user's needs.

Electrochemical impedance spectroscopy (EIS), cyclic voltammetry (CV) and galvanostatic charge/discharge (GCD) are the most known methods for obtaining the parameters used in the characterization of supercapacitors. In accordance with IEC standard [9], the capacitance of a double-layer capacitor can be calculated through the discharge curve after a charge-rest-discharge procedure. Several authors uses GCD method to determine capacitance and equivalent series resistance (ESR) of supercapacitors and it has been widely accepted [4]. Raut, A. S. [6] highlights the feasibility of the GCD method in determining the power and energy densities of supercapacitors electrodes. This method can also be used to verify how close to the ideal is the behavior of the supercapacitor through the potential against time linearity [10].

It is evident the versatility of the GCD method as a tool for the characterization of supercapacitors. Basically, the GCD technique involves the use of a constant positive current to charge the device to a defined potential, then the device is discharged by a constant negative current. During the charge and discharge cycles, time and potential are recorded. From the discharge curve, it is possible to calculate capacitance, energy density and the power density of the device. By repeating this procedure for different discharge times, it is possible to construct a Ragone plot, which is widely used for comparing relative performance between energy storage devices [2, 4, 6, 11]. The stability of the capacitor is evaluated by performing a series of charge and discharge cycles, in which the capacitance retention is observed as a function of cycle number. Typically, this experiment involves thousands of cycles making it favorable to use a system.

In this work, we developed a supercapacitor characterization system using Lua scripting, a programable sourcemeter and a two-electrode electrochemical cell. This system uses the galvanostatic charge/discharge method to acquire the main parameters for the characterization of supercapacitor electrode materials.

2. Results and Discussion

Script description

Figure 1 shows the main algorithm of the capacitor characterization system. In this algorithm, the main loop controls the number of test cycles, which can be defined through the variable ncycle for the GCD mode or adding a series of currents when opting for the Ragone plot mode. Within each cycle, current and voltage measurements are made, the set current is applied, and the voltage is monitored until the maximum voltage value (stopv) is reached. Then the current source is inverted, the voltage is monitored until startv is achieved, and the discharge time is stored (dt). At the end of each cycle, the capacitance is calculated by the ratio between the discharge current and the slope of the discharge curve (stopv/dt). From the discharge current, discharge time, mass of active material, capacitance, specific capacitance, energy density and power density are calculated for each charge and discharge cycle. The results are printed in a properly formatted text block for subsequent graphing.

Figure 2 shows the partial report generated after a GCD test. The report header displays the parameters used in the test. In this specific case, a potential window of 0.4 V, charge and discharge current of 0.001 A, the total mass of active material of 32 mg and 5 charge and discharge cycles were used. The report also presents three columns of data: The first one shows the elapsed time; the second shows the current applied; and the third one the measured potential. These data are used to construct the charge and discharge curves, as shown in Figure 3. Another important section of the report is shown in Figure 2 (b), where capacitance and specific capacitance are recorded for each charge and discharge cycle performed. These data are used to construct the stability plot. It is important to note that in the case of measurements made on commercial capacitors there is no need to include the mass of the active material and the specific capacitance result should be ignored.

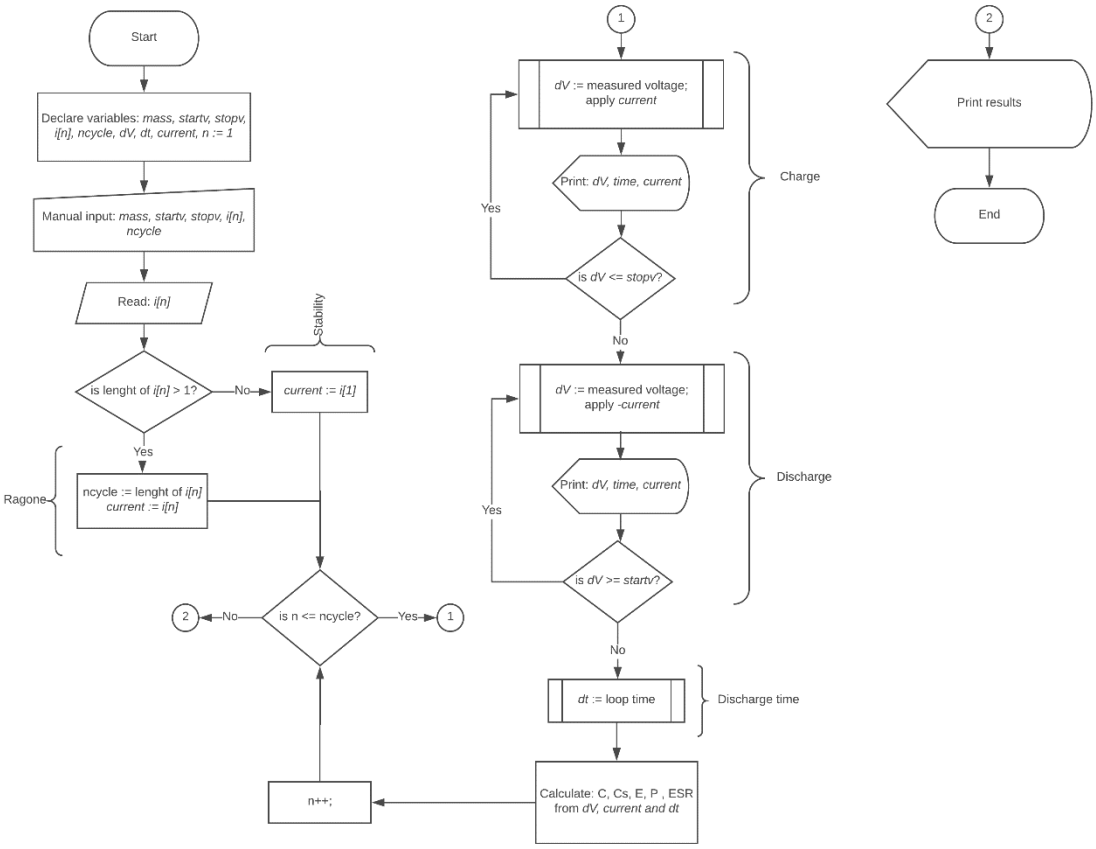

Figure 1. Main algorithm of the supercapacitors characterization system.

a)

```
--- CHARGE DISCHARGE CURVE ---
Sample: Activated carbon
Date: 20/10/17
Electrode mass: 0.032g
Voltage range: 0V to 0.4V
Current: 0.001A

Time            Current         Voltage
s               A               V
6.91601e-01     9.99986e-04     1.42095e-02
7.92301e-01     9.99984e-04     1.59702e-02
8.92933e-01     9.99966e-04     1.73164e-02
```

b)

	Cycle	Capacitance F	Specific Capacitance F/g
1	1.00000e+00	2.05245e-01	2.56557e+01
2	2.00000e+00	2.13336e-01	2.66670e+01
3	3.00000e+00	2.19613e-01	2.74516e+01
4	4.00000e+00	2.24887e-01	2.81109e+01
5	5.00000e+00	2.29928e-01	2.87409e+01

	Voltage drop V	ESR Ohms	Discharge Time s
1	2.56117e-02	2.56117e+01	8.21191e+01
2	2.56034e-02	2.56034e+01	8.53433e+01
3	2.55930e-02	2.55930e+01	8.78532e+01
4	2.56087e-02	2.56087e+01	8.99677e+01
5	2.56704e-02	2.56704e+01	9.19788e+01

Figure 2. (a) Partial report of the galvanostatic charge/discharge mode and (b) table of calculated results for each charge/discharge cycle.

Figure 3 shows the GCD curve plotted from the data obtained in the GCD report for the activated carbon electrode. The specific capacitance was calculated from the slope of the discharge curve in the region between 80% and 40% of the maximum voltage [12]. The specific capacitance values calculated and provided by the script are shown in Table 1. The specific capacitance value is sensitive to small variations in the slope of the discharge curve. For example, for the activated carbon electrode used in this study, a slope of -0.003 represented a specific capacitance of 41.67 F/g, while a slope of -0.004 represented 31.25 F/g. By comparing the calculated values from the graph with those calculated by the system, we could assume that there was good agreement between them. The advantage of the system is related to the reproducibility of the method, avoiding errors related to some possible arbitrariness that may occur in the selection of the region where the calculation is going to be made. In addition, when a very large number of cycles

are performed, the manual calculation becomes unfeasible.

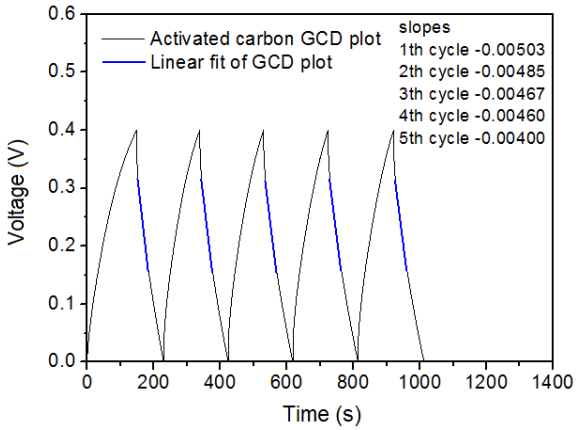

Figure 3. Galvanostatic charge-discharge curve of an activated carbon electrode in 6 M KOH electrolyte showing the slopes of each cycle in the region between 80% and 40% of the maximum voltage.

Table 1. Specific capacitance calculated and generated by the GCD script for the activated carbon electrode.

Cycle number	Calculated Csp (F/g)	Script generated Csp (F/g)
1	24.85	25.66
2	25.77	26.67
3	26.77	27.45
4	27.17	28.11
5	31.25	28.74

System validation

In addition to the specific capacitance measurements of the supercapacitor using a two-electrode cell, capacitance measurements were also performed using commercial capacitors of 100, 1000, 4700 and 10000 µF with the aim of validating the system. These results are presented in Table 2.

Table 2. Capacitance in Farads obtained in five charge and discharge cycles for capacitors of 100, 1000, 4700, and 10000 µF.

Cycle number	Capacitance (F)			
	100 µF capacitor	1000 µF capacitor	4700 µF capacitor	10000 µF capacitor
1	$1.040x10^{-4}$	$1.000x10^{-3}$	$4.800x10^{-3}$	$1.009x10^{-2}$
2	$1.043x10^{-4}$	$1.010x10^{-3}$	$4.830x10^{-3}$	$1.014x10^{-2}$
3	$1.046x10^{-4}$	$1.010x10^{-3}$	$4.840x10^{-3}$	$1.007x10^{-2}$
4	$1.037x10^{-4}$	$1.000x10^{-3}$	$4.850x10^{-3}$	$1.009x10^{-2}$
5	$1.039x10^{-4}$	$1.000x10^{-3}$	$4.860x10^{-3}$	$1.011x10^{-2}$

The average values of capacitance obtained by the characterization system for commercial capacitors of 100, 1000, 4700 and 10000 µF were $1.04x10^{-4}$, $1.01x10^{-3}$, $4.83x10^{-3}$ and $1.01x10^{-2}$ F, respectively. The difference between the experimental and specification values was 4% for the 100 µF capacitor; 1% for the 1000 µF capacitor; 2.8% for the 4700 µF capacitor, and 1% for the 10000 µF capacitor. The differences for all capacitors were within the tolerance range of commercial capacitors, which could be up to 20% [13]. The data presented in Table 2 also demonstrates the excellent reproducibility of measurements, which is most evident by observing the stability results shown in Figure 5 (a).

Figure 4 (a) shows 500 charge and discharge cycles performed on commercial capacitors. This result demonstrated the characteristic that the capacitors present in retaining their storage capacity even after several cycles of charge and discharge. The plot also demonstrated the efficiency of the system in the attainment of this type of curve, which is fundamental in the characterization of new materials that are capable of storing energy. This plot is also important for the characterization of pseudocapacitive supercapacitors, as the charge retention must be demonstrated in these types of devices, since the charge storage mechanism involves redox reactions and may undergo changes during the stability tests [14–16]. EIS measurements were also performed on the commercial capacitors for comparison purposes. The results are in the Bode plot shown in Figure 4 (b). The capacitance values obtained at the frequency of 0.01 Hz are displayed on the graph and are also within the tolerance range.

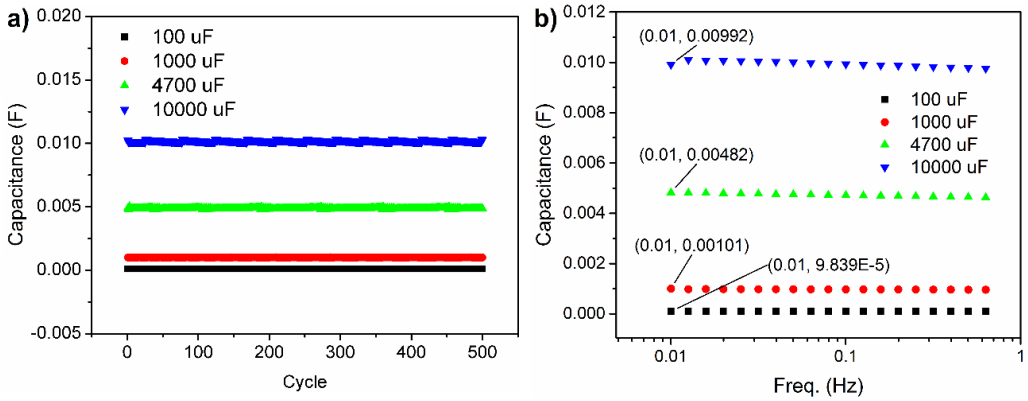

Figure 4. (a) Capacitance in Farads vs. cycles number for commercial capacitors of 100, 1000, 4700 and 10000 µF. (b) Bode plot in the low-frequency region for commercial capacitors tested.

Both methods are effective in determining the capacitance of ESDs, however, the system proposed here stands out for stability measurements with several charge/discharge cycles, as it minimizes the time for testing and data processing.

Figure 5 (a) and (b) shows SEM images of the electrode surfaces before and after electrodeposition treatment. In the electrodeposited sample, the presence of MnO_2 is clearly observed and is consistent with those presented in other studies [10, 17, 18]. The EDS result shown in Figure 5 (b) indicate the presence of this phase on the surface of the nickel foam. The coating with manganese oxide had a strong influence on the capacitance values obtained by both GCD and CV. The capacitance calculated from the GCD curves generated by the program were very close to those presented in the GCD curves. The small difference shown is related to the region of the curve selected for the calculation of capacitance, since the data used for the calculations are the same. Figure 5 (e) shows the results obtained by CV for the NF and NF-MnO_2 samples, respectively. Obviously, the effect presented by MnO_2 was also observed in the CV results. Comparing the capacitance values obtained in both techniques, both are in the same order of magnitude. It is well known that the scan rate affects the capacitance values and that for a non-ideal capacitor, the capacitance value depends on the applied potential. These particularities justify the small differences obtained between the two techniques used. The results of both techniques were similar, justifying the applicability of the proposed system in pseudocapacitive electrodes.

The script used to construct the Ragone plot is similar to the one used for the GCD test, since the values of energy density and power density were obtained during the discharge of the capacitor. As seen in the previous section, the user report the test currents and the program perform charge and discharge cycles on each of the defined currents. During the device discharge, the capacitance, specific capacitance, energy density, current density, voltage drop and ESR are calculated. The time and discharge current are also recorded.

Figure 6 (a) presents the report generated for the elaboration of the Ragone plot and Figure 6 (b) shows the GCD curves with progressive currents used to generate the Ragone plot of the activated carbon supercapacitor. As expected, the discharge time decreased with increasing current density. The current density also had an influence on the specific capacitance, which increased with lower current values. This is a typical behavior of supercapacitors and is attributed to a better ion accessibility in the porous structure of the active material [19, 20]. The inset graph of Figure 6 (b) highlights the manually calculated ESR for the current density cycle of 0.25 A/g. The value was the same as that generated by the characterization system, as shown in Figure 6 (a). Since the ESR has great influence on the loss of energy, this is a parameter that should be minimized during the design of the ESDs [12]. The Ragone mode presented here facilitated the determination of ESR and can be used both in the research and in the characterization of new materials used in energy storage devices.

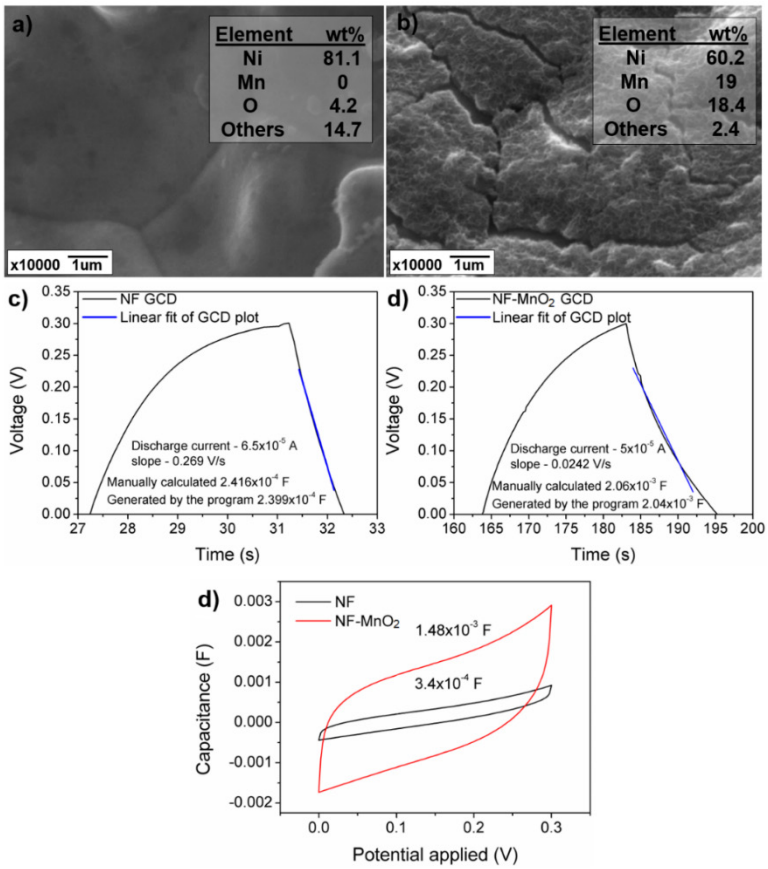

Figure 5. (a) and (b) Ni foam (NF) surface as-received and electrodeposited (NF-MnO_2), respectively. (c) and (d) GCD plots of NF and NF-MnO_2 electrodes, respectively. (e) Voltammograms of NF and NF-MnO_2 electrodes at a scan rate of 50 mV/s.

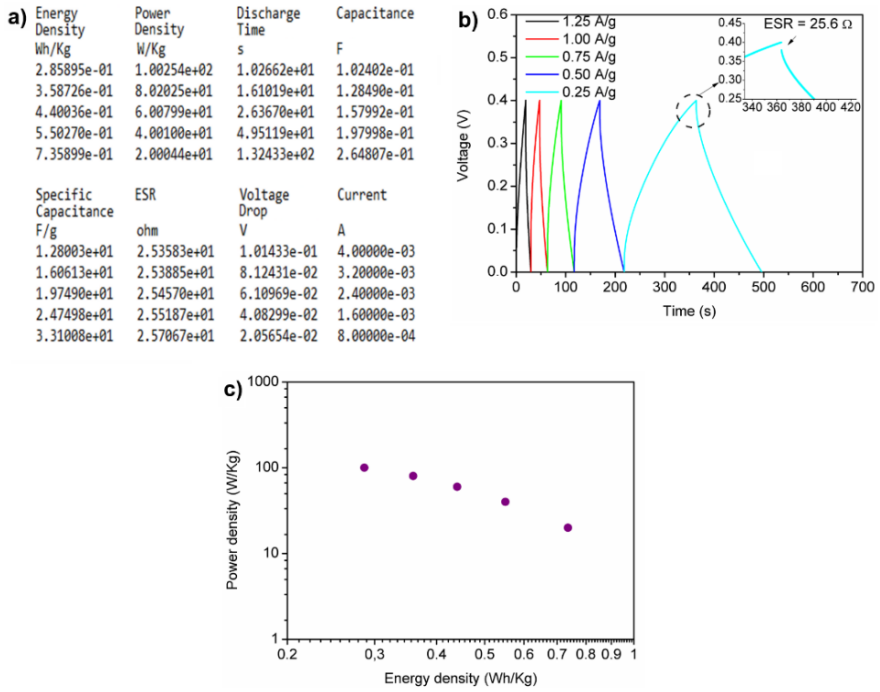

Figure 6. Report generated for the Ragone mode after testing with the activated carbon supercapacitor. (b) GCD plot with various current densities used in calculations of energy density and power density. (c) Ragone plot of activated carbon supercapacitor.

Figure 6 (c) shows the Ragone plot obtained from the GCD script. It was possible to observe that for this supercapacitor; the energy density decreased significantly with the increase in the power density. This effect may be related to the series resistance of the cell used in the test [21]. The energy density varied between 0.29 and 0.74 Wh/Kg while the power density varied from 20 to 100 W/Kg for the 5 currents used. These values were consistent with those reported in the literature for similar systems [22,23]. It should be noted that higher energy values can be obtained with the use of pseudocapacitive active materials, such as transition metal oxides and conductive polymers [24,25]. Activated carbon was used during the simulations to demonstrate the feasibility of using this system for any application in the supercapacitor area.

3. Material and Methods

The capacitor characterization system was developed to obtain the necessary data for plotting Ragone, GCD and stability curves. The main system script was written in Lua scripting language using the development platform Test Script Builder® (TSB), Keithley Instruments, with the following functions: galvanostatic charge-discharge, capacitor stability and Ragone plot. The instrument used for the tests was a programmable sourcemeter Keithley model 2651A with current resolution up to 100 fA.

System validation

System validation was performed by running the script on commercial capacitors of 100, 1000, 4700 and 10000 µF. Capacitance measurements were carried out through the galvanostatic charge/discharge script. Stability tests were also performed to verify the reproducibility of measurements and capacitor stability. Electrochemical impedance spectroscopy was also carried out on all commercial capacitors for comparison purposes. Ragone plot mode was performed using a two-electrode cell, represented in Figure 7, with current collectors made of 304 stainless steel. Activated carbon was used as active material, KOH 6M as electrolyte, Nafion® as a binder and filter paper as separator.

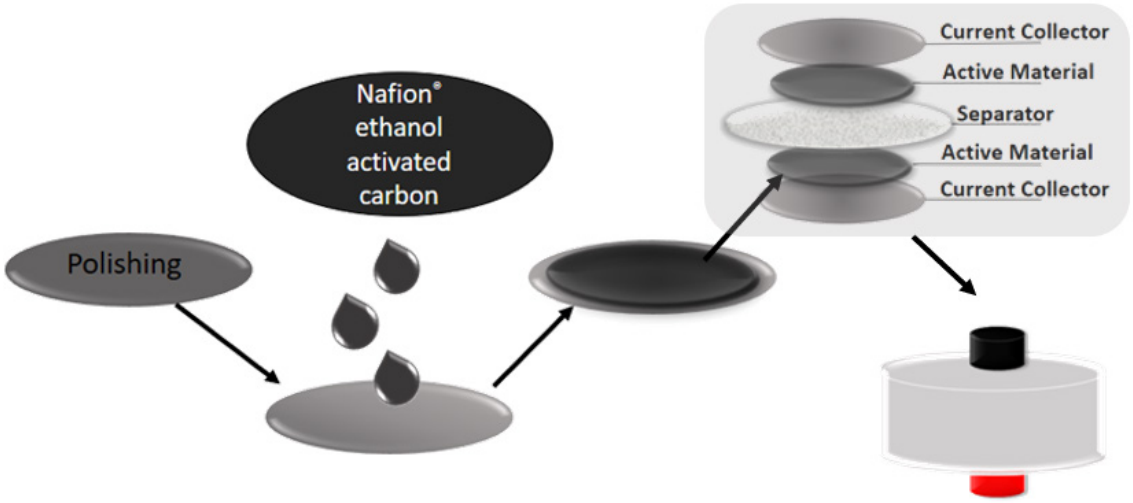

Figure 7. Schematic representation of activated carbon electrode preparation process and the two-electrode cell assembly used in the charge-discharge measurements.

The electrode preparation was performed using the following procedure, as shown in Figure 7. The current collector surfaces were ground and finished with 1200-grit abrasive paper and subjected to ultrasonic cleaning in acetone, ethyl alcohol and distilled water (30 minutes with each solvent). A solution containing 50 µl of Nafion®, 3 ml ethyl alcohol and 40 mg activated carbon was dispersed in ultrasound for 120 minutes. Then the solution was carefully added on the surface of the current collectors until a thin uniform layer of the electrode material was formed. Finally, the electrodes were dried overnight at 60 °C.

In addition, charge and discharge

measurements were performed using the characterization system in pseudo-capacitive electrodes. The capacitance values obtained were compared with those obtained by cyclic voltammetry performed using an autolab potentiostat running Nova 2.1.2 software. The electrodes used in this step were nickel foam and nickel foam electrodeposited with manganese oxide, respectively. Manganese oxide is a well-known pseudo-capacitive material and was deposited according to the method described by Hu, L. and coworkers [17].

Data measurement and calculations

The galvanostatic charge/discharge method was used as basis for developing the capacitor characterization system. By means of this technique, the capacitance is calculated from the discharge curve by using the following equation:

$$C = I_{dc}/(dV/dt) \quad (1)$$

where C is the capacitance, I_{dc} is the discharge current and dV/dt is the slope of the discharge curve. The specific capacitance (C_{sp}) is calculated by C_{sp} = 4C/m, where m is the total mass of the active material [26]. Since there is an equivalent series resistance (ESR) present in the device, which includes the electrode, electrolyte and cell connections resistors, the system was programmed to calculate the capacitance after the voltage drop (IR drop) that occurs at the beginning of the discharge. The ESR was also recorded in the script output report and was calculated by the following equation:

$$ESR = V_{drop}/-I_{dc} \quad (2)$$

For Ragone curves, the system calculated the energy density (E) and the power density (P) from the discharging capacitance by means of the following equations:

$$E = 1/2\ C_{sp}\ V^2 \quad (3)$$

and

$$P = E/\Delta t \quad (4)$$

respectively, where V is the voltage window and Δt is the discharge time.

4. Conclusions

The capacitor characterization system was efficient and easy to operate. With the insertion of a few number of variables it was possible to obtain a set of data capable of completely and efficiently characterizing new materials and devices used in the research and development of energy storage devices. The great advantage of using a programmable sourcemeter as a research and development tool for supercapacitors was the versatility of building and modifying characterization techniques. The system was able to determine the capacitance of the tested devices with results similar to those obtained by EIS and CV. The system proved to be effective in determining the stability of the ESDs after several charge/discharge cycles, whose determination by EIS is impracticable and by CV requires a special care in data processing. Automation of measurements, reproducibility of results, and reliability of calculations are a part of this program. It is worth noting that we are not proposing the substitution of the traditional electrochemical characterization techniques that are extremely important in the characterization of the materials used in electrodes, but an alternative way of obtaining the main parameters used to characterize energy storage devices.

Acknowledgments

The authors gratefully acknowledge with thanks, the financial support of FAPERGS/PqG 2017 under number 17/2551-0001157-0, and CAPES/PROCAD 2013/2998/2014. The authors declare no competing financial interest.

References and Notes

[1] Snook, G. A.; Kao, P.; Best, A. S. *J. Power Sources* **2011**, *19*, 1. [Crossref]

[2] Simon, P.; Gogotsi, Y. *Nat. Mater.* **2008**, *7*, 845. [Crossref]

[3] Eng, A. Y. S.; Chua, C. K.; Pumera, M. *Phys. Chem. Chem. Phys.* **2016**, *18,* 9673 [Crossref]

[4] Stoller, M. D.; Ruoff, R. S. *Energy Environ. Sci.* **2010**, *3*, 1294. [Crossref]

[5] Lajnef, W.; Vinassa, J. M.; Briat, O.; Azzopardi, S.; Woirgard, E. *J. Power Sources* **2007**, *168*, 553. [Crossref]

[6] Raut, A. S.; Parker, C. B.; Glass, J. T. *J. Mater. Res.* **2010**, *25*, 1500. [Crossref]

[7] Clark, D. L. *AUTOTESTCON (Proceedings)* **2009**. [Crossref]

[8] Marujoa, R. de F. B.; Fonseca, L. M. G.; Körtinga, T. S.; do Nascimento Bendinia, H.; de Queiroza, G. R.; Vinhas, L.; Ferreiraa, K. R. *J. Comp. Int. Sci*. **2017**, *3*, 8. [Crossref]

[9] International Electrotechnical Comission International Standard IEC 62391-1:2015 2006. [Link]

[10] Ding, K. Q. *J. Chinese Chem. Soc.* **2009**, *56*, 175. [Crossref]

[11] Wang, W.; Guo, S.; Lee, I.; Ahmed, K.; Zhong, J.; Favors, Z.; Zaera, F.; Ozkan, M.; Ozkan, C. S. *Sci. Rep*. **2014**, *4*, 1. [Crossref]

[12] Lehtimäki, S.; Railanmaa, A.; Keskinen, J.; Kujala, M.; Tuukkanen, S.; Lupo, D. *Sci. Rep.* **2017**, *7*. [Link]

[13] Haghnazari, S.; Zolghadri, M. R. A novel voltage measurement technique for modular multilevel converter capacitors. In *IECON 2015 - 41st Annual Conference of the IEEE Industrial Electronics Society*; 2015. [Crossref]

[14] Christinelli, W. A.; Gonçalves, R.; Pereira, E. C. *Electrochim. Acta* **2016**, *196*, 741. [Crossref]

[15] Evanko, B.; Yoo, S. J.; Chun, S. E.; Wang, X.; Ji, X.; Boettcher, S. W.; Stucky, G. D. *J. Am. Chem. Soc.* **2016**, *138*, 9373. [Crossref]

[16] Gu, T.; Wei, B. *Nanoscale* **2015**, *7*, 11626. [Crossref]

[17] Hu, L.; Chen, W.; Xie, X.; Liu, N.; Yang, Y.; Wu, H.; Yao, Y.; Pasta, M.; Alshareef, H. N.; Cui, Y. *ACS Nano* **2011**, *5*, 8904. [Crossref]

[18] Kim, E. K.; Shrestha, N. K.; Lee, W.; Cai, G.; Han, S. H. *Mater. Chem. Phys.* **2015**, *155*, 211. [Crossref]

[19] Qie, L.; Chen, W.; Xu, H.; Xiong, X.; Jiang, Y.; Zou, F.; Hu, X.; Xin, Y.; Zhang, Z.; Huang, Y. *Energy Environ. Sci.* **2013**, *6*, 2497. [Crossref]

[20] Kou, L.; Huang, T.; Zheng, B.; Han, Y.; Zhao, X.; Gopalsamy, K.; Sun, H.; Gao, C. *Nat. Commun.* **2014**, *5*, 1. [Crossref]

[21] An, K. H.; Kim, W. S.; Park, Y. S.; Moon, J. M.; Bae, D. J.; Lim, S. C.; Lee, Y. S.; Lee, Y. H. *Adv. Funtional Mater.* **2001**. [Crossref]

[22] Ruiz, V.; Blanco, C.; Santamaría, R.; Ramos-Fernández, J. M.; Martínez-Escandell, M.; Sepúlveda-Escribano, A.; Rodríguez-Reinoso, F. *Carbon* **2009**, *47*, 195. [Crossref]

[23] Qu, Q. T.; Shi, Y.; Tian, S.; Chen, Y. H.; Wu, Y. P.; Holze, R. *J. Power Sources* **2009**, *194,* 1222. [Crossref]

[24] Lee, H. J.; Lee, J. H.; Chung, S. Y.; Choi, J. W. *Angew. Chemie - Int. Ed.* **2016**, 55, 3958. [Crossref]

[25] Deng, W.; Ji, X.; Chen, Q.; Banks, C. E. *RSC Adv.* **2011**, *1*, 1171. [Crossref]

[26] Gan, J. K.; Lim, Y. S.; Huang, N. M.; Lim, H. N. *Appl. Surf. Sci.* **2015**, *357*, 479. [Crossref]